

Protein–Surfactant Film Voltammetry of Wild-Type and Mutant Cytochrome P450 BM3

Andrew K. Udit,[†] Nareen Hindoyan,[‡] Michael G. Hill,[‡] Frances H. Arnold,[†] and Harry B. Gray*[†]

Division of Chemistry and Chemical Engineering, California Institute of Technology, Pasadena, California 91125, and Department of Chemistry, Occidental College, Los Angeles, California 90041

Received November 17, 2004

We are investigating the redox chemistry of wild-type (WT) and mutant (1-12G) cytochrome P450 BM3. Absorption spectra in solution feature the Fe^{III} Soret at 418 nm for WT and a split Soret for 1-12G at 390 and 418 nm. Voltammetry of the proteins within DDAPSS films on the surface of carbon electrodes reveal nearly identical Fe^{III/II} potentials (approximately –200 mV vs Ag/AgCl), but significant differences in k° , 250 vs 30 s^{–1}, and Fe^{III/II}–CO potentials, –140 vs –115 mV, for WT vs 1-12G. Catalytic reduction of dioxygen by the proteins on rotating-disk electrodes was analyzed using Levich and Koutecky–Levich treatments. The data reveal 1-12G n and k_{obs} values that are, respectively, 1.7 and 0.07 times those of WT, suggesting that the two proteins differ strikingly in their reactions with dioxygen.

The cytochromes P450 (P450s) catalyze challenging oxidation reactions under physiological conditions.¹ Interest in these proteins stems not only from their biological importance (e.g., xenobiotic elimination),² but also from their ability to perform valuable industrial reactions (e.g., alkane hydroxylation).^{3,4} The P450 isolated from *Bacillus megaterium*, cytochrome P450 BM3, has received significant attention because of its high turnover rates and its similarity to the relatively little-understood mammalian forms.⁵ In recent years, it has been demonstrated that this protein can tolerate a number of mutations, creating variants with enhanced or even novel activities.^{6,7}

We are investigating the redox chemistry of the heme domains of wild-type cytochrome P450 BM3 (WT) and mutant 1-12G (1-12G). The 15 mutations that distinguish 1-12G from WT are collectively responsible for 1-12G's unique catalytic properties, which include the ability to regio- and stereoselectively hydroxylate linear hydrocarbons [e.g., formation of (*S*)-2-octanol at 40% ee] and oxidize small gaseous alkanes (e.g., propane).⁷ Conceivably, these differences in catalysis might be due in part to differences in redox properties. Previous work with WT has shown that single-point mutations can significantly perturb the heme's redox and catalytic properties.⁸ We suspected that the 15 mutations in 1-12G would have a similar effect: indeed, one of the distinguishing features of 1-12G is that, as isolated (heme domain, substrate free), the heme is mixed-spin (absorption at 390 and 418 nm). This is in stark contrast to WT (Figure 1), which shows the characteristic low-spin absorption spectrum of a hydrated six-coordinate heme ($\lambda_{\text{max}} = 418$ nm).

To compare the redox chemistry of these two proteins, we made protein films on the surface of carbon electrodes using the surfactant–polyanion film didodecyltrimethylammonium polystyrenesulfonate (DDAPSS). Heme proteins within DDAPSS films have been shown to retain their solution spectroscopic properties and are active toward dioxygen reduction and reductive dehalogenation.^{9,10} We note that previous work reported the redox properties of WT in DDAB;¹¹ this serves as a convenient point of reference for the present investigation of WT and 1-12G in DDAPSS.

Protein films for voltammetry were cast on the surface of basal-plane graphite electrodes (BPG). The two proteins were found to give similar voltammograms; $E_{1/2}$ values for WT

* To whom correspondence should be addressed. E-mail: hbgray@caltech.edu.

[†] California Institute of Technology.

[‡] Occidental College.

- (1) Ortiz de Montellano, P. R., Ed. *Cytochrome P450: Structure, Mechanism, and Biochemistry*, 2nd ed.; Plenum Press: New York, 1995.
- (2) Guengerich, F. P. *Mol. Interventions* **2003**, *3*, 194–204.
- (3) Urlacher, V. B.; Lutz-Wahl, S.; Schmid, R. D. *Appl. Microbiol. Biotechnol.* **2004**, *64*, 317–325.
- (4) van Beilen, J. B.; Duetz, W. A.; Schmid, A.; Witholt, B. *Trends Biotechnol.* **2003**, *21*, 170–177.
- (5) Munro, A.; Leys, D.; McLean, K.; Marshall, K.; Ost, T.; Daff, S.; Miles, C.; Chapman, S.; Lysek, D.; Moser, C.; Page, C.; Dutton, P. *Trends Biochem. Sci.* **2002**, *27*, 250–257.

- (6) Glieder, A.; Farinas, E. T.; Arnold, F. H. *Nat. Biotechnol.* **2002**, *20*, 1135–1139.
- (7) Peters, M. W.; Meinhold, P.; Glieder, A.; Arnold, F. H. *J. Am. Chem. Soc.* **2003**, *125*, 13442–13450.
- (8) Ost, T. W. B.; Clark, J.; Mowat, C. G.; Miles, C. S.; Walkinshaw, M. D.; Reid, G. A.; Chapman, S. K.; Daff, S. *J. Am. Chem. Soc.* **2003**, *125*, 15010–15020.
- (9) Ma, H.; Hu, N. *Anal. Lett.* **2001**, *34*, 339–361.
- (10) Blair, E.; Greaves, J.; Farmer, P. J. *J. Am. Chem. Soc.* **2004**, *126*, 8632–8633.
- (11) Fleming, B. D.; Tian, Y.; Bell, S. G.; Wong, L.; Urlacher, V.; Hill, H. A. O. *Eur. J. Biochem.* **2003**, *270*, 4082–4088.

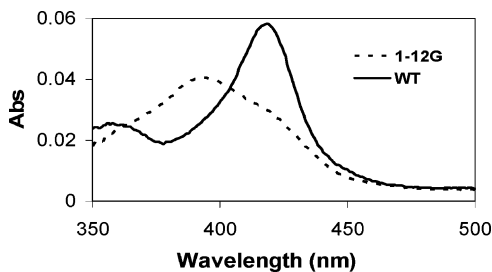


Figure 1. Absorption spectra of WT and 1-12G P450 BM3 in the absence of substrate.

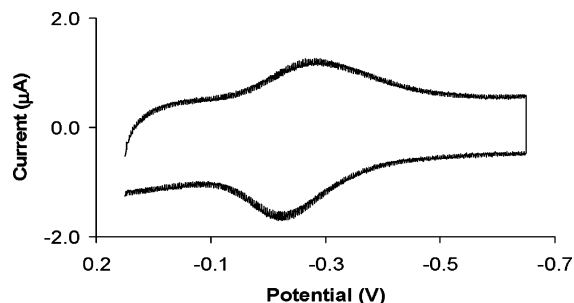


Figure 2. Cyclic voltammogram of mutant 1-12G in DDAPSS on BPG at 200 mV/s in 50 mM KP/20 mM KCl/pH 7.

and 1-12G are -195 and -202 mV, respectively. A representative voltammogram at pH 7 for 1-12G in DDAPSS is shown in Figure 2. We have assigned the couple in Figure 2 to heme $\text{Fe}^{\text{III/II}}$, consistent with other studies^{12–14} and in accord with WT in DDAB (cf. -250 mV vs SCE¹¹). Notably, the potentials are shifted by approximately $+370$ mV compared to the WT enzyme in solution (six-coordinate heme, low-spin).¹⁵ Empirically, potential shifts of this magnitude are usually observed for heme proteins in surfactant films;¹⁶ the hydrophobic film likely leads to partial heme dehydration, resulting in the positive potential shift.¹⁷

For both proteins, the peak currents are linear with scan rate (surface-bound) up to 14 V/s, after which they become linear with the square root of the scan rate (diffusive).¹⁸ This is characteristic of thin-film electrochemistry,¹⁹ indicative of finite diffusion of the protein within the film. Thus, up to 14 V/s, the systems can be treated as surface-confined. Within this diffusionless regime, the ratios of the total charge under the cathodic and anodic peaks ($Q_{p,c}/Q_{p,a}$) approach unity for both proteins, indicating chemically reversible systems.¹⁸

Voltammetry in the presence of carbon monoxide revealed a notable difference in the $\text{Fe}^{\text{III/II}}$ potentials of WT

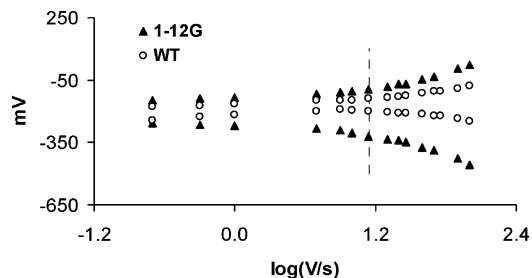


Figure 3. Cathodic and anodic peak potentials vs logarithm of the scan rate for WT and 1-12G. The vertical line represents the transition from surface-bound to diffusive behavior.

(-140 mV) and 1-12G (-115 mV) (see Supporting Information, Figure S1). Approximately, this indicates a 4-fold difference in $\text{Fe}^{\text{III/II}}$ –CO binding affinities between WT and 1-12G in the DDAPSS film and provides further evidence that the two proteins have different heme environments.

Figure 3 presents a plot of the peak potentials vs the logarithm of the scan rate for both proteins. Despite nearly identical $\text{Fe}^{\text{III/II}}$ potentials, Figure 3 demonstrates that the two proteins differ significantly in their electron-transfer (ET) properties. Within the diffusionless regime (Figure 3, vertical line), the theory of Laviron can be used to estimate the standard rate constant k° ($\Delta G^{\circ} = 0$).²⁰ Assuming a transfer coefficient (α) of 0.5, k° values at 10 V/s are 250 and 30 s^{-1} for WT and 1-12G, respectively. (Notably, k° for WT in DDAB¹¹ is 221 s^{-1} .)

Voltammograms of the two proteins in the presence of dioxygen resulted in catalytic currents at the onset of Fe^{III} reduction. The stability of DDAPSS films to mechanical stress⁹ permitted the use of a rotating-disk electrode (RDE) to investigate the dioxygen reaction. The diffusion–convection-limited current at an RDE depends on the angular rotational velocity (ω , s^{-1}), the number of electrons transferred (n), and the bulk concentration of substrate (O_2 in this case) according to the Levich equation^{21,22}

$$i_L = 0.62nFA^{2/3}[\text{O}_2]v^{-1/6}\omega^{1/2}$$

RDE experiments were carried out on both WT and 1-12G by performing electrolysis at -0.5 V (vs Ag/AgCl) and measuring the limiting current for each rotation rate. These data points are plotted in Figure 4 (points), along with theoretical lines for two- and four-electron reductions of dioxygen (solid lines).

For both proteins, the limiting currents in Figure 4 appear to level off at high rotation rates. This indicates that dioxygen reduction is limited by a chemical step preceding the electrode reaction. The Koutecký–Levich treatment was used to analyze the kinetics;²³ plots of i_L^{-1} vs $\omega^{-1/2}$ were linear

- (12) Zhang, Z.; Nassar, A.-E.; Lu, Z.; Schenkman, J. B.; Rusling, J. F. *J. Chem. Soc., Faraday Trans.* **1997**, *93*, 1769–1774.
 (13) Rusling, J. F.; Nassar, A.-E. *F. J. Am. Chem. Soc.* **1993**, *115*, 11891–11897.
 (14) Immoos, C. E.; Chou, J.; Bayachou, M.; Blair, E.; Greaves, J.; Farmer, P. J. *J. Am. Chem. Soc.* **2004**, *126*, 4934–4942.
 (15) Daff, S.; Chapman, S.; Turner, K.; Holt, R.; Govindaraj, S.; Poulos, T.; Munro, A. *Biochemistry* **1997**, *36*, 13816–13823.
 (16) Lvov, Y. M.; Lu, Z.; Schenkman, J. B.; Zu, X.; Rusling, J. F. *J. Am. Chem. Soc.* **1998**, *120*, 4073–4080.
 (17) Tezcan, F. A.; Winkler, J. R.; Gray, H. B. *J. Am. Chem. Soc.* **1998**, *120*, 13383–13388.
 (18) Bard, A. J.; Faulkner, L. R. *Electrochemical Methods*, 2nd ed.; John Wiley & Sons: New York, 2001.
 (19) Lin, R.; Immoos, C. E.; Farmer, P. J. *J. Biol. Inorg. Chem.* **2000**, *5*, 738–747.

- (20) Laviron, E. *J. Electroanal. Chem.* **1979**, *101*, 19–28.
 (21) Levich, V. *Physicochemical Hydrodynamics*; Prentice Hall: Englewood Cliffs, NJ, 1962.
 (22) F is Faraday's constant, A is the electrode area (cm^2), D is the diffusion coefficient (1.7×10^{-5} cm^2/s for oxygen in water), v is the kinematic viscosity of the solution (0.01 cm^2/s for water), $[\text{O}_2] = 2.9 \times 10^{-7}$ mol/cm^3 for O_2 in air-saturated buffer at 20 °C.
 (23) Koutecký, J.; Levich, V. *Zh. Fiz. Khim.* **1956**, *32*, 1565.

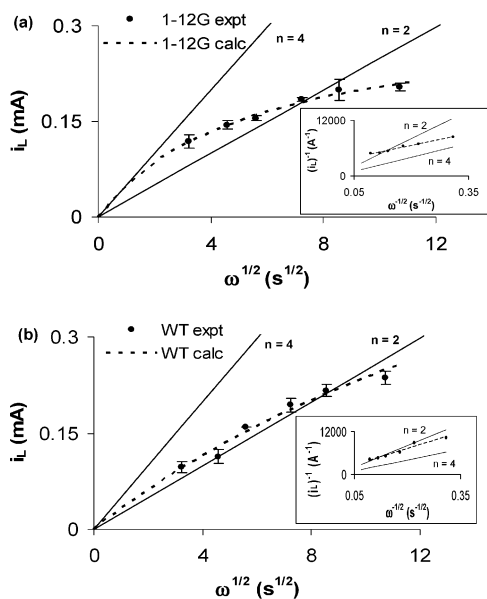


Figure 4. Levich plots for (a) 1-12G and (b) WT. The individual points, solid lines, and broken lines represent the experimental data, theoretical lines, and lines derived from the fit of the experimental data, respectively. The insets are the corresponding Koutecky–Levich plots, from which n and k_{obs} were derived. The O_2 concentration used to generate the lines, $2.9 \times 10^{-7} \text{ mol/cm}^3$, is that of air-saturated buffer at 20°C .

for both proteins, with slopes yielding $n = 2.7$ for WT and $n = 4.7$ for 1-12G (insets, Figure 4). The intercepts of the Koutecky–Levich plots were used to calculate the kinetic currents (i_{kin}) that limit the electrode reaction. These currents vary linearly with protein concentration and are given by²⁴

$$i_{\text{kin}} = nFA[\text{O}_2]\Gamma_{\text{P450}}k_{\text{obs}}$$

(where Γ_{P450} is the surface concentration of protein and k_{obs} is the second-order rate constant that governs the current-limiting reaction). WT and 1-12G gave values for k_{obs} of 1.4×10^6 and $1 \times 10^5 \text{ M}^{-1} \text{ s}^{-1}$, respectively, a 14-fold difference in reaction rate. The calculated values for n and k_{obs} were used to generate Levich plots for WT and 1-12G (Figure 4, broken lines).

Chemical fates of dioxygen reduction are one-, two-, and four-electron transfers, forming superoxide, peroxide, and water, respectively. Our calculated values for n are probably overestimated: dioxygen is likely more concentrated within the hydrophobic film than in solution.²⁵ With this in mind, it appears that WT reduces dioxygen primarily by two electrons to peroxide (as seen before for WT and BM3 point mutants^{11,26}), whereas 1-12G apparently reduces dioxygen by an additional two electrons. P450-catalyzed four-electron reduction of dioxygen has been previously observed^{6,27} and

(24) Andrieux, C.; Saveant, J.-M. *Molecular Design of Electrode Surfaces*; Wiley & Sons: New York, 1992.

(25) Using $[\text{O}_2] = 3.3 \times 10^{-7} \text{ mol/cm}^3$ results in n values of 4.1 and 2.3 for 1-12G and WT, respectively.

is consistent with the canonical P450 mechanism that results in water formation by reducing compound I with two electrons (“oxidase” activity).²⁸ Dioxygen reduction by 1-12G is also significantly slower (k_{obs}) compared to that by WT, as evident from the prominent plateau at higher rotation rates for 1-12G where the rate of substrate delivery exceeds that of catalysis.

Results from our electroanalytical treatment can be correlated with the biochemistry of the proteins. First, there is the 10-fold difference in heterogeneous ET rate constants (k°). Indeed, preliminary stopped-flow experiments using holo proteins and NADPH as the reductant revealed that heme reduction in WT occurs approximately 5-fold faster.²⁹ In addition, substrate turnover rates for WT³⁰ are generally faster (up to 10-fold) than for 1-12G;⁷ given that ET is known to be the rate-limiting step, the relative k° and k_{obs} values are also consistent with the catalytic oxidation rates. Second, there is the striking observation that, under similar conditions, 1-12G appears to be capable of reducing dioxygen by four electrons. This difference can be reconciled if the iron-peroxy species is longer lived in 1-12G. For WT, peroxide apparently dissociates before subsequent conversion to compound I. However, the lower rate of ET in 1-12G, coupled with the observation of catalytic currents corresponding to four-electron transfer to dioxygen, argues for an iron-peroxy complex that is longer-lived in 1-12G than in WT. This could potentially explain the high degree of stereo- and regioselectivity that 1-12G displays: a longer-lived iron-peroxy species allows substrates more time to adopt their lowest-energy conformation within the active site and orient a specific C–H bond for subsequent hydroxylation. This argument is in accord with that previously postulated for 1-12G,⁷ which reasoned that the mutations (especially A328V and A82L in the active site) keep the substrate in a more fixed orientation, allowing specific products to be generated.

Acknowledgment. E. Blair and P. J. Farmer (UC Irvine) for assistance with film preparation; M. W. Peters and P. Meinhold (Caltech) for helpful discussions; and NSERC (Canada) (A.K.U.), NIH (H.B.G.), and the David and Lucille Packard Foundation (M.G.H.) for research support.

Supporting Information Available: Voltammograms of WT and 1-12G in CO-saturated buffer; details on protein purification, voltammetry, and RDE experiments. This material is available free of charge via the Internet at <http://pubs.acs.org>.

IC0483747

(26) Noble, M.; Miles, C.; Chapman, S.; Lysek, D.; Mackay, A.; Reid, G.; Hanzlik, R.; Munro, A. *Biochem. J.* **1999**, *339*, 371–379.

(27) Kadkhodayan, S.; Coulter, E. D.; Maryniak, D. M.; Bryson, T. A.; Dawson, J. H. *J. Biol. Chem.* **1995**, *270*, 28042–28048.

(28) Wong, L. L.; Westlake, C. G.; Nickerson, D. P. In *Structure and Bonding*; Springer-Verlag: Berlin, 1997; Vol. 88, pp 175–207.

(29) Shoo, J.; Meinhold, P.; Peters, M. W. California Institute of Technology, **2004**, Unpublished results.

(30) Boddupalli, S.; Estabrook, R.; Peterson, J. *J. Biol. Chem.* **1990**, *265*, 4233–4239.